GBA1 deficiency negatively affects physiological α-synuclein tetramers and related multimers

Sangjune Kim[a,b,1], Seung Pil Yun[a,b,c,1], Saebom Lee[a,b], George Essien Umanah[a,b], Veera Venkata Ratnam Bandaru[a,b], Xiling Yin[a,b,c], Peter Rhee[a,b], Senthilkumar S. Karuppagounder[a,b], Seung-Hwan Kwon[a], Hojae Lee[a,b], Xiaobo Mao[a,b,c], Donghoon Kim[a,b], Akhilesh Pandey[d,e], Gabsang Lee[a,b,f], Valina L. Dawson[a,b,c,f,g], Ted M. Dawson[a,b,c,f,h], and Han Seok Ko[a,b,c,i,2]

[a]Neuroregeneration and Stem Cell Programs, Institute for Cell Engineering, The Johns Hopkins University School of Medicine, Baltimore, MD 21205; [b]Department of Neurology, The Johns Hopkins University School of Medicine, Baltimore, MD 21205; [c]Adrienne Helis Malvin Medical Research Foundation, New Orleans, LA 70130; [d]Mckusick-Nathans Institute of Genetic Medicine, The Johns Hopkins University School of Medicine, Baltimore, MD 21205; [e]Department of Biological Chemistry, The Johns Hopkins University School of Medicine, Baltimore, MD 21205; [f]Solomon H. Snyder Department of Neuroscience, The Johns Hopkins University School of Medicine, Baltimore, MD 21205; [g]Department of Physiology, The Johns Hopkins University School of Medicine, Baltimore, MD 21205; [h]Department of Pharmacology and Molecular Sciences, The Johns Hopkins University School of Medicine, Baltimore, MD 21205; and [i]Diana Helis Henry Medical Research Foundation, New Orleans, LA 70130

Edited by Gregory A. Petsko, Weill Cornell Medical College, New York, NY, and approved December 8, 2017 (received for review January 9, 2017)

Accumulating evidence suggests that α-synuclein (α-syn) occurs physiologically as a helically folded tetramer that resists aggregation. However, the mechanisms underlying the regulation of formation of α-syn tetramers are still mostly unknown. Cellular membrane lipids are thought to play an important role in the regulation of α-syn tetramer formation. Since glucocerebrosidase 1 (GBA1) deficiency contributes to the aggregation of α-syn and leads to changes in neuronal glycosphingolipids (GSLs) including gangliosides, we hypothesized that GBA1 deficiency may affect the formation of α-syn tetramers. Here, we show that accumulation of GSLs due to GBA1 deficiency decreases α-syn tetramers and related multimers and increases α-syn monomers in CRISPR-GBA1 knockout (KO) SH-SY5Y cells. Moreover, α-syn tetramers and related multimers are decreased in N370S *GBA1* Parkinson's disease (PD) induced pluripotent stem cell (iPSC)-derived human dopaminergic (hDA) neurons and murine neurons carrying the heterozygous L444P *GBA1* mutation. Treatment with miglustat to reduce GSL accumulation and overexpression of GBA1 to augment GBA1 activity reverse the destabilization of α-syn tetramers and protect against α-syn preformed fibril-induced toxicity in hDA neurons. Taken together, these studies provide mechanistic insights into how GBA1 regulates the transition from monomeric α-syn to α-syn tetramers and multimers and suggest unique therapeutic opportunities for PD and dementia with Lewy bodies.

GBA1 | α-synuclein | tetramers | glucosylceramide | Parkinson's disease

Misfolding and pathogenic aggregation of α-synuclein (α-syn) have been implicated in familial and sporadic Parkinson's disease (PD) and other α-synucleinopathies (1, 2). It has long been believed that α-syn exists as a natively unfolded monomer and belongs to the class of intrinsically disordered proteins that lack an organized secondary structure (3). Therefore, α-syn monomer tends to readily aggregate and convert into β-sheet oligomers and eventually into insoluble amyloid-like deposits such as Lewy bodies (LB). However, the N-terminal region of α-syn contains a lipid-binding domain that allows α-syn to adopt an amphipathic helix structure upon binding to synaptic and other vesicles that contain acidic phospholipids (4). Importantly, certain missense mutations in the N-terminal domain of α-syn observed in early onset familial PD lead to impaired membrane binding in vitro and in yeast (4, 5). Although the physiological role of α-syn is unclear, some evidence suggests that it is involved in the exocytic process (6) and recycling of synaptic vesicles as well as in the regulation of synaptic transmission by forming membrane-bound helical multimers (7, 8).

Under physiological conditions, an intracellular pool of α-syn is found in a dynamic equilibrium between a free monomeric species and a membrane-bound multimeric conformation depending on the cellular environment (1, 2). Recent studies indicate that α-syn physiologically exists as a folded helical tetramer that resists aggregation (9, 10). The transition from tetramer to monomer is increased by PD α-syn missense mutations located in the lipid-binding motif (11). Furthermore, the importance of the lipid-binding motif has been confirmed by the observation that overexpression of wild-type α-syn constructs with substitutions in the canonical α-syn repeat motifs (KTKEGV) that disrupt lipid binding increases the levels of unfolded monomer, round-shaped inclusions, and neuronal toxicity (12). Together, these studies indicate a crucial role of the lipid-binding motif in the formation of tetramers, suggesting that lipid composition in the membrane may regulate tetramer formation.

Glucocerebrosidase 1 (GBA1) is a lysosomal hydrolase that cleaves glucosylceramide (GlcCer) to glucose and ceramide (13). Mutations in the *GBA1* gene are recognized as a strong risk factor for the development of PD and dementia with Lewy bodies (DLB) (14, 15). GBA1 loss-of-function mutations exhibit lower GBA1 enzymatic activity and increase accumulation of lipid substrates in the lysosome and thereby compromise lysosomal activity (16–19). Importantly, intracellular GlcCer levels control the formation of soluble toxic α-syn assemblies in neuronal cultures, mouse, and

Significance

Recent studies have identified a helically folded tetramer as the major normal structure of α-synuclein (α-syn) and that the tetramer resists aggregation. However, the underlying mechanisms that regulate the formation of α-syn tetramers remain elusive. Our study shows that mutations in glucocerebrosidase 1 (*GBA1*) and depletion-induced GBA1 deficiency leading to accumulation of glycosphingolipids (GSLs) are sufficient to cause destabilization of α-syn tetramers and increase the susceptibility of human dopaminergic neurons to cytotoxicity due to exposure to pathologic α-syn fibrils. Therefore, maintaining GBA1 activity and reducing GSLs are potentially important in reducing misfolding and pathogenic aggregation of α-syn in Parkinson's disease.

Author contributions: S.K., S.P.Y., and H.S.K. designed research; S.K., S.P.Y., S.L., G.E.U., V.V.R.B., X.Y., S.S.K., and H.L. performed research; S.P.Y., S.L., S.-H.K., X.M., and D.K. contributed new reagents/analytic tools; S.K., S.P.Y., V.V.R.B., A.P., G.L., V.L.D., T.M.D., and H.S.K. analyzed data; and S.K., S.P.Y., V.V.R.B., P.R., V.L.D., T.M.D., and H.S.K. wrote the paper.

The authors declare no conflict of interest.

This article is a PNAS Direct Submission.

[1]S.K. and S.P.Y. contributed equally to this work.

[2]To whom correspondence should be addressed. Email: hko3@jhmi.edu.

This article contains supporting information online at www.pnas.org/lookup/suppl/doi:10.1073/pnas.1700465115/-/DCSupplemental.

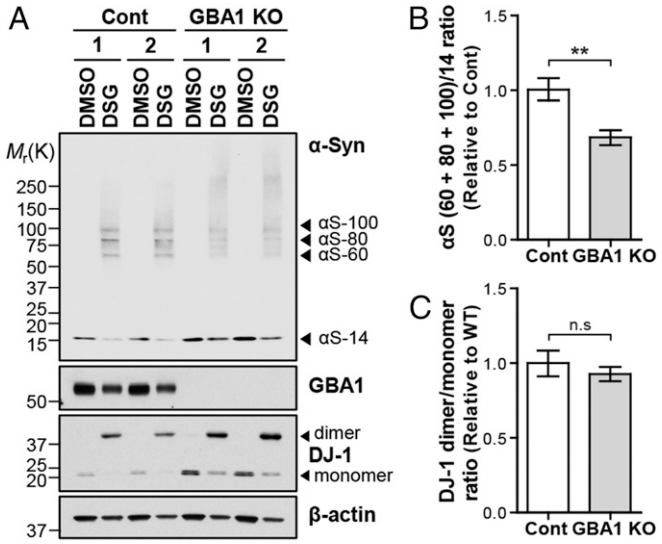

Fig. 1. α-Syn tetramers and related multimers in SH-SY5Y cells with GBA1 KO by the CRISPR/Cas9 system. (*A*) Cytosolic fractions from 1 mM DSG–cross-linked control and GBA1 KO cells were analyzed by Western blot using anti–α-Syn antibody to detect cross-linked α-syn. αS, α-synuclein. (*B*) Quantification of the cytosolic αS60 + 80 + 100:14 ratio in the GBA1 KO cells relative to the ratio in the control cells ($n = 6$). (*C*) Quantification of the ratio of DJ-1 dimer to monomer ($n = 6$). The error bars represent SEM. $^{**}P < 0.01$; n.s., not significant.

human brain, leading to neurodegeneration (20). In addition, GlcCer hampers lysosome–autophagy fusion and thereby blocks degradation of lysosomal proteins, leading to accumulation of α-syn and neurotoxicity (21). Since GBA1 deficiency induced glycosphingolipid (GSL) accumulation and soluble toxic α-syn assemblies are tightly interconnected (20), it is likely that GBA1 deficiency could affect the formation of α-syn helical multimers. To address this possibility, we investigated whether accumulation of GSLs due to GBA1 deficiency disrupts the formation of α-syn tetramers and related multimers in clustered, regularly interspaced short palindromic repeats (CRISPR)/CRISPR-associated 9 (Cas9)-GBA1 KO cells (hereafter noted as GBA1 KO) and heterozygous N370S GBA1-PD induced pluripotent stem cell (iPSC)-derived human dopaminergic (hDA) neurons. Here, we report that accumulation of intracellular GSLs due to GBA1 deficiency is important for destabilizing normal α-syn tetramers/multimers and making soluble toxic α-syn assemblies.

Results

Depletion of GBA1 Leads to Destabilization of α-Syn Tetramers and Related Multimers. To explore whether GBA1 deficiency could affect the formation of α-syn tetramers and related multimers, we generated human neuroblastoma SH-SY5Y cell lines with depletion of GBA1 using the CRISPR/Cas9 system without any desirable off-target effects (*SI Appendix*, Fig. S1*A*). These GBA1 KO cells lead to no detectable levels of GBA1 protein, RNA and enzymatic activity, and the subsequent accumulation of α-syn in both whole-cell lysates and lysosome-enriched fractions (*SI Appendix*, Fig. S1). Consistent with prior studies using GBA1-depleted cells (20, 21), depletion of GBA1 results in accumulation of lysosomal associated membrane protein 1 (LAMP-1) but not the endoplasmic reticulum (ER) stress marker, 78 kDa glucose-regulated protein (GRP78), suggesting that depletion of GBA1 contributes to lysosomal dysfunction but not to ER stress (*SI Appendix*, Fig. S1*B*). Since it is difficult to distinguish between the α-syn monomer and helical tetramers using native gel electrophoresis (22), we employed an intact cell cross-linking method that allows detection of the α-syn tetramers with 1 mM disuccinimidyl glutarate (DSG), a membrane-permeable cross-linker, as previously described (11, 12). Since detergents for cell lysis could profoundly affect destabilization of the tetramers, GBA1 KO cells were lysed by sonication as previously described (23). In the GBA1 KO cells, the cross-linked α-syn tetramers (60 kDa) and related multimers (80 and 100 kDa) are decreased, whereas the amount of free monomer is increased compared with control cells (Fig. 1 *A* and *B* and *SI Appendix*, Fig. S2). Similar results are observed in primary cortical neurons carrying the heterozygous L444P *GBA1* mutation (*SI Appendix*, Fig. S3), the most common *GBA1* mutation in neuronopathic Gaucher disease (GD) (14, 15). α-Syn 60-, 80-, and 100-kDa species (tetramers/multimers) detected in cells are different from the soluble toxic oligomer species, because soluble oligomeric species of α-syn could only be detected in cells overexpressing α-syn (*SI Appendix*, Fig. S4). To confirm cross-linking efficiency, dimerization of DJ-1 was assessed in DSG-treated lysates as a positive control (23, 24). DJ-1 is efficiently associated into a homodimer. Unexpectedly, dimeric and monomeric DJ-1 forms are increased, whereas the ratio of DJ-1 dimer to monomer is not altered in GBA1 KO cells compared with control cells (Fig. 1*C* and *SI Appendix*, Fig. S2).

Accumulation of GSLs Due to GBA1 Deficiency Reduces the Ratio of α-Syn Tetramers and Related Multimers to Monomers. GBA1 deficiency primarily leads to pathological accumulation of GSLs in the lysosome due to loss of GBA1 enzymatic activity (18, 20). Importantly,

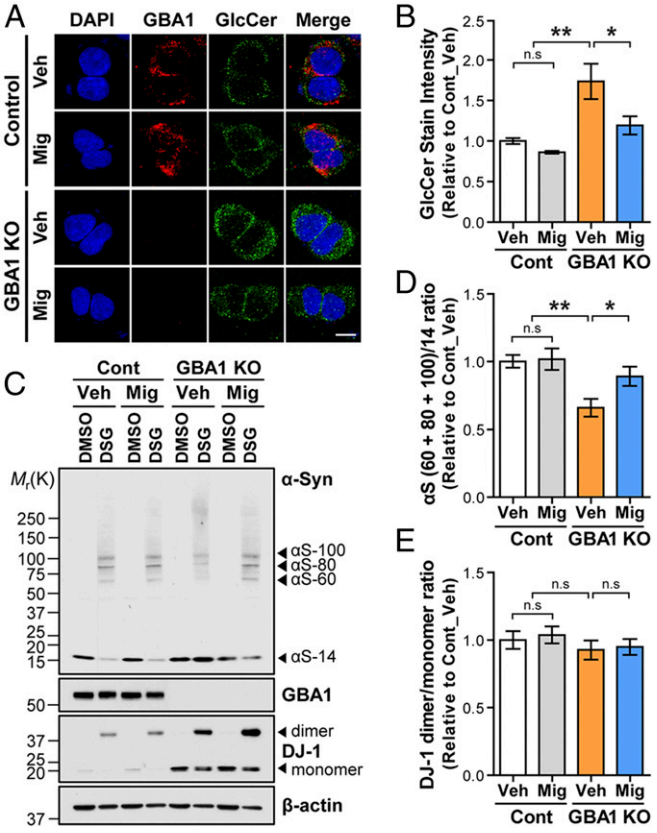

Fig. 2. Rescue effects of GSL reducing agent on GSL homeostasis and formation of α-syn tetramers and related multimers. (*A*) Fluorescent microscopic images of vehicle or 100 μM miglustat treatment for 3 d in control and GBA1 KO cells using anti-GBA1 and anti-GlcCer antibodies. (Scale bar, 10 μm.) (*B*) Quantification of GlcCer intensity divided by number of DAPI-stained cells relative to vehicle-treated control cells ($n = 4$). (*C*) Cytosolic fractions of DSG–cross-linked control and GBA1 KO cells with or without miglustat treatment. (*D*) Quantification of the α-syn multimers to monomer ratio for *C* ($n = 6$). (*E*) Quantification of the ratio of DJ-1 dimer to monomer ($n = 6$). The error bars represent SEM. $^{*}P < 0.05$; $^{**}P < 0.01$; n.s., not significant.

lipid-binding motifs of α-syn protein are thought to be critical for the formation of tetramers and related multimers (11). To examine whether accumulation of GSLs due to GBA1 deficiency influences levels of α-syn tetramers, we assessed the relationship between intracellular GlcCer levels and α-syn tetramer levels in the presence or absence of miglustat, an inhibitor of GlcCer synthase (25). Consistent with previous studies in GBA1-deficient cells (18), GBA1 KO cells have a 1.73-fold and 2.37-fold increase in intracellular GlcCer levels as assessed by immunofluorescence analysis for anti-GlcCer antibody and quantitative lipidomics analysis, whereas treatment with 100 μM miglustat results in a reduction in the levels of intracellular GlcCer to near-normal status (Fig. 2 *A* and *B* and *SI Appendix*, Fig. S5 *A* and *B*). Total ceramide levels are not significantly but slightly decreased in GBA1 KO cells (*SI Appendix*, Fig. S5 *C* and *D*), whereas its species composition shows a similar pattern in both control and GBA1 KO cells treated with or without miglustat (*SI Appendix*, Fig. S5 *E* and *F*). Importantly, the GBA1 deficiency-induced reduction of tetramers and related multimers is significantly recovered by treatment with miglustat in GBA1 KO cells (Fig. 2 *C* and *D*), but the ratio of DJ-1 dimer to monomer is not altered (Fig. 2*E*). Together, these data suggest that GSL accumulation due to GBA1 deficiency contributes to the destabilization of α-syn tetramers and related multimers.

Generation of hDA Neurons from GBA1-PD Patients. To extend our findings, we generated hDA neurons carrying a *GBA1* mutation. To this end, PD patient skin fibroblasts harboring the *GBA1* mutation (N370S/WT GBA1-PD) were obtained from Coriell (*SI Appendix*, Table S1) and reprogrammed using standard techniques (26). Immunostaining analysis with control and GBA1-PD iPSC lines shows expression of alkaline phosphatase (AP) and pluripotency protein markers (*SI Appendix*, Fig. S6*A*). No differences are observed in the levels of protein and RNA of pluripotency markers between all iPSC and human embryonic stem cells (H9) (*SI Appendix*, Fig. S6 *B–D*). Furthermore, we confirmed normal euploid karyotypes (*SI Appendix*, Fig. S6*E*) and the formation of teratomas (*SI Appendix*, Fig. S6*F*). Importantly, all iPSC-derived hDA neurons show a similar differentiation potential (*SI Appendix*, Fig. S7 *A–D*) and comparable protein and RNA levels of neuronal and hDA markers including tyrosine hydroxylase (TH), TUJ1, MAP2, PITX3, Nurr1, and FOXA2 (*SI Appendix*, Fig. S7 *E–G*). Notably, no significant differences are observed in dopamine release (*SI Appendix*, Fig. S8*A*) and electrophysiological properties among hDA neurons differentiated from control and GBA1-PD iPSC lines (*SI Appendix*, Fig. S8 *B–H*).

Reduction in GBA1 Protein Levels and Activity as Well as Accumulation of GSLs and α-Syn in hDA Neurons Harboring a *GBA1* Mutation. Since reduction in GBA1 protein levels and activity are a feature of sporadic PD and GBA1-PD (27), we determined GBA1 protein levels and enzyme activity and α-syn levels in PD patient fibroblasts, iPSC, neuronal precursors, and hDA neurons. GBA1 protein levels and enzyme activity are profoundly reduced in all of these cells with the *GBA1* N370S mutation compared with control-derived cells (Fig. 3 *A* and *B* and *SI Appendix*, Figs. S9 and S10*A*). These results are similar to the finding in postmortem PD brains carrying a heterozygous *GBA1* mutation and hDA neurons differentiated from iPSC harboring a heterozygous *GBA1* mutation (16, 28). As described previously (17), α-syn protein is only detected in iPSC and neuronal precursors, and the protein levels are higher in GBA1-PD iPSC and neuronal precursors compared with control (*SI Appendix*, Fig. S9 *D*, *E*, *G*, and *H*). Interestingly, the level of α-syn protein is markedly higher in hDA neurons differentiated from GBA1-PD iPSC compared with hDA neurons differentiated from the controls (Fig. 3*A* and *SI Appendix*, Fig. S10*B*), whereas the level of TH protein is not changed in all hDA neurons (Fig. 3*A* and *SI Appendix*, Fig. S10*C*), suggesting that *GBA1* N370S perturbs α-syn processing (Fig. 3*A* and *SI Appendix*, Fig. S10*B*). Intriguingly, α-syn protein is not detected in fibroblasts (*SI Appendix*, Fig. S9*A*). Next, GSL levels were assessed via liquid chromatography mass spectrometry (LC-MS) using hDA neurons at 60 d in vitro (DIV 60) (29). The analysis shows a 1.87-fold increase in GBA1–PD1-1 and a 2.08-fold increase in GBA1-PD2 compared with control hDA neurons (Fig. 3*C* and *SI Appendix*, Fig. S11*A*). Interestingly, total ceramide levels are slightly decreased in both GBA1–PD1-1 and GBA1-PD2 compared with controls (Fig. 3*D* and *SI Appendix*, Fig. S11*B*), whereas ceramide species composition

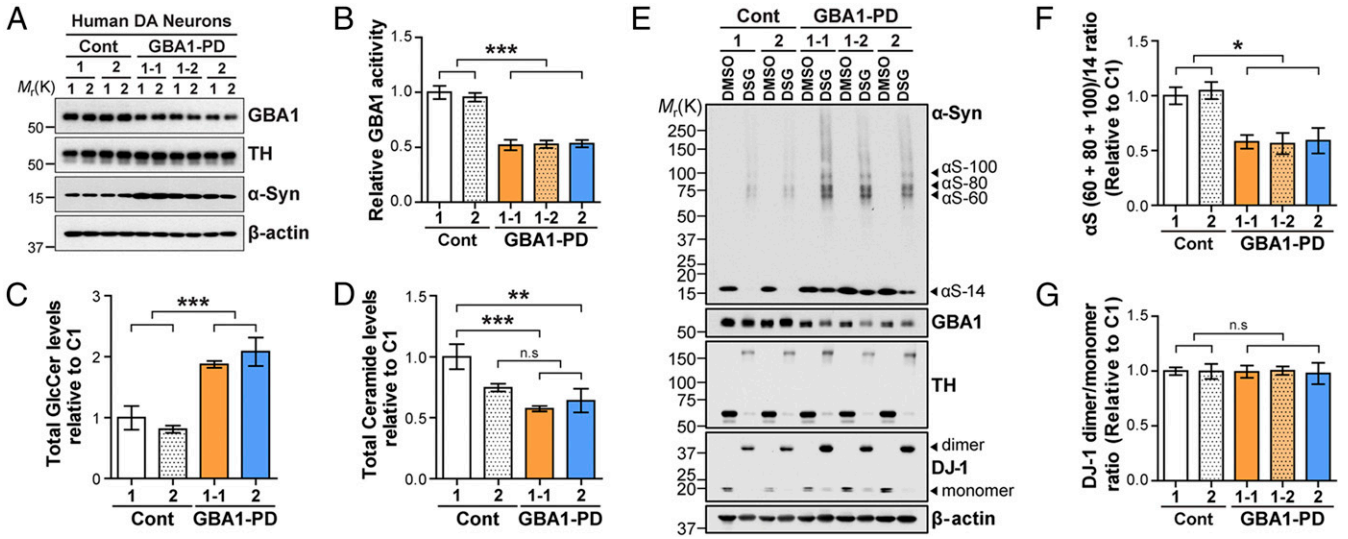

Fig. 3. GBA1 protein levels and enzyme activity as well as GlcCer levels and the formation of α-syn tetramers and related multimers in GBA1-PD iPSC-derived hDA neurons. (*A*) GBA1, α-syn, and TH protein levels in hDA neurons were analyzed by Western blot using anti-GBA1, anti–α-Syn, and anti-TH antibodies. TH, tyrosine hydroxylase. (*B*) The GBA1 enzymatic activities were measured using lysosome-enriched fractions in control and GBA1-PD hDA neurons. GBA1 enzyme activity was quantified and normalized to the control ($n = 6$). (*C*) GlcCer and (*D*) ceramide levels from DIV 60 control and GBA1-PD hDA neurons were measured using MS, and values are quantified as relative to those measured in control hDA neurons ($n = 3$). (*E*) Cytosolic fractions of 1 mM DSG–cross-linked DIV 60 control and GBA1-PD hDA neurons were analyzed by Western blot using anti–α-Syn, anti-GBA1, anti-TH, anti–DJ-1, and anti–β-actin antibodies. (*F*) Quantification of the α-syn multimers to monomer ratio for *E* ($n = 4$). (*G*) Quantification of the ratio of DJ-1 dimers to monomer for *E* ($n = 4$). The error bars represent SEM. $^*P < 0.05$; $^{**}P < 0.01$; $^{***}P < 0.001$; n.s., not significant.

shows a similar pattern among these hDA neurons (*SI Appendix*, Fig. S11 *C* and *D*). Since accumulated GlcCer levels were observed, we sought to determine whether the accumulation of GlcCer alters the ratio of α-syn tetramers and related multimers to free monomers. Strikingly, DSG cross-linking analysis using hDA neurons reveals that the ratios of α-syn tetramers and related multimers to free monomers are significantly decreased in all GBA1-PD–derived hDA neurons, suggesting that destabilization of the tetramers and related multimers is correlated with the levels of GlcCer (Fig. 3 *E* and *F*). No difference is observed in the ratio of DJ-1 dimer to monomer (Fig. 3 *E* and *G*) and in the ratio of TH tetramers to monomers between GBA1-PD and control hDA neurons (Fig. 3*E*).

Miglustat Treatment or Augmentation of GBA1 Protein Stabilizes the Formation of α-Syn Tetramers and Related Multimers in hDA Neurons. Since our findings demonstrate that GlcCer accumulation destabilizes the α-syn tetramers and related multimers, which subsequently leads to accumulation of the free monomer of α-syn in GBA1-PD hDA neurons, we next sought to determine whether miglustat could increase α-syn tetramers and related multimers in GBA1-PD hDA neurons through reducing GlcCer synthesis. For effective inhibition of GlcCer synthesis, hDA neurons were treated with 100 μM miglustat as the concentration did not affect the GBA1 protein levels and enzyme activity as well as TH protein levels (*SI Appendix*, Fig. S12). DSG–cross-linking analysis shows that treatment with miglustat significantly reverses the destabilization of the α-syn tetramers and related multimers due to GBA1 deficiency-mediated GSL accumulation as assessed by Western blot analysis (Fig. 4 *A* and *B*). Similarly, augmentation of GBA1 protein via lentiviral transduction also recovers the ratio of α-syn tetramers and related multimers to monomers (Fig. 4 *D* and *E*). Interestingly, the increases in DJ-1 level due to GBA1 deficiency are decreased in GBA1-overexpressed GBA1-PD hDA neurons (Fig. 4*D*) but not miglustat-treated GBA1-PD hDA neurons (Fig. 4*A*). On the other hand, the ratio of DJ-1 dimer to monomer is similar in both miglustat-treated and GBA1-overexpressed GBA1-PD hDA neurons compared with control hDA neurons (Fig. 4 *C* and *F*). No differences in TH protein levels and the ratio of TH tetramers to monomer are observed in all groups (Fig. 4 *A* and *D*).

Miglustat Protects Against PFF-Induced Toxicity in hDA Neurons. We then determined whether reduced free monomers of α-syn by miglustat treatment rescues the pathology induced by preformed fibrils (PFF) (30). To this end, control and GBA1-PD hDA neurons at DIV 60 were treated with 100 μM miglustat 3 d before PFF treatment (5 μg/mL). Ten days after PFF treatment, the levels of phospho-Ser129 α-syn (p-α-syn), a marker for pathologic α-syn, are significantly increased in GBA1-PD hDA neurons with vehicle treatment, while treatment of miglustat significantly decreases the levels of p-α-syn in GBA1-PD hDA neurons as assessed by immunofluorescence analysis with anti–p-α-syn antibody (Fig. 5 *A* and *B*). For further analysis of the levels of p-α-syn, the control and GBA1-PD hDA neurons were fractionated into Triton X-100 (TX)-soluble and -insoluble fractions. TH levels are decreased in both control and GBA1-PD hDA neurons with PFF treatment in TX-soluble fractions. Notably, the reduction in TH levels are greater in GBA1-PD hDA neurons treated with PFF compared with that in control hDA neurons treated with PFF (Fig. 5*C* and *SI Appendix*, Fig. S10*E*). Importantly, the reduction in TH levels is partially but significantly recovered in both control and GBA1-PD hDA neurons by treatment of miglustat in the TX-soluble fraction (Fig. 5*C* and *SI Appendix*, Fig. S10*E*). However, endogenous α-syn levels are unchanged and p-α-syn levels are barely detectable in the TX-soluble fraction (Fig. 5*C* and *SI Appendix*, Fig. S10*D*). Importantly, PFF treatment leads to accumulation of abnormal α-syn aggregate species (Fig. 5*D* and *SI Appendix*, Fig. S10*F*) and an increase in the level of p-α-syn (Fig. 5*D* and *SI Appendix*, Fig. S10*G*) in the TX-insoluble fraction in both control and GBA1-PD hDA neurons, whereas miglustat reduces the accumulation of the TX-insoluble α-syn aggregate species (Fig. 5*D* and *SI Appendix*, Fig. S10*F*) and p-α-syn (Fig. 5*D* and *SI Appendix*, Fig. S10*G*). On the other hand, the accumulation in α-syn aggregate species and p-α-syn levels in the TX-insoluble fraction is greater in GBA1-PD hDA neurons treated with PFF compared with those in PFF-treated control hDA neurons. Next, we monitored neuronal toxicity induced

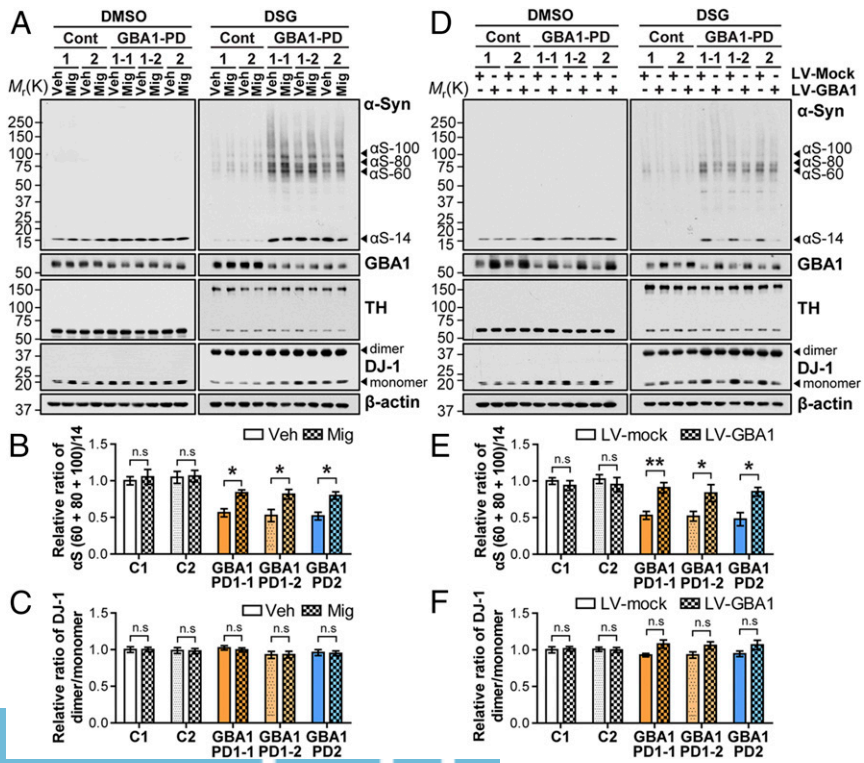

Fig. 4. The formation of α-syn tetramers and related multimers in GBA1-PD iPSC-derived hDA neurons with miglustat treatment and lentiviral GBA1 transduction. (*A*) Cytosolic fractions of 1 mM DSG–cross-linked control and GBA1-PD hDA neurons with or without 100 μM miglustat treatment for 3 d were analyzed by Western blot using anti–α-Syn, anti-GBA1, anti-TH, anti–DJ-1, and anti–β-actin antibodies. (*B*) Quantification of the α-syn multimers to monomer ratio for *A* ($n = 4$). (*C*) Quantification of the ratio of DJ-1 dimers to monomer for *A* ($n = 4$). (*D*) Cytosolic fractions of 1 mM DSG–cross-linked control and GBA1-PD hDA neurons with LV-mock or LV-GBA1 viral transduction for 5 d were analyzed by Western blot analysis. (*E*) Quantification of the α-syn multimers to monomer ratio for *D* ($n = 3$). (*F*) Quantification of the ratio of DJ-1 dimers to monomer levels for *D* ($n = 3$). The error bars represent SEM. $^*P < 0.05$; $^{**}P < 0.01$; n.s., not significant.

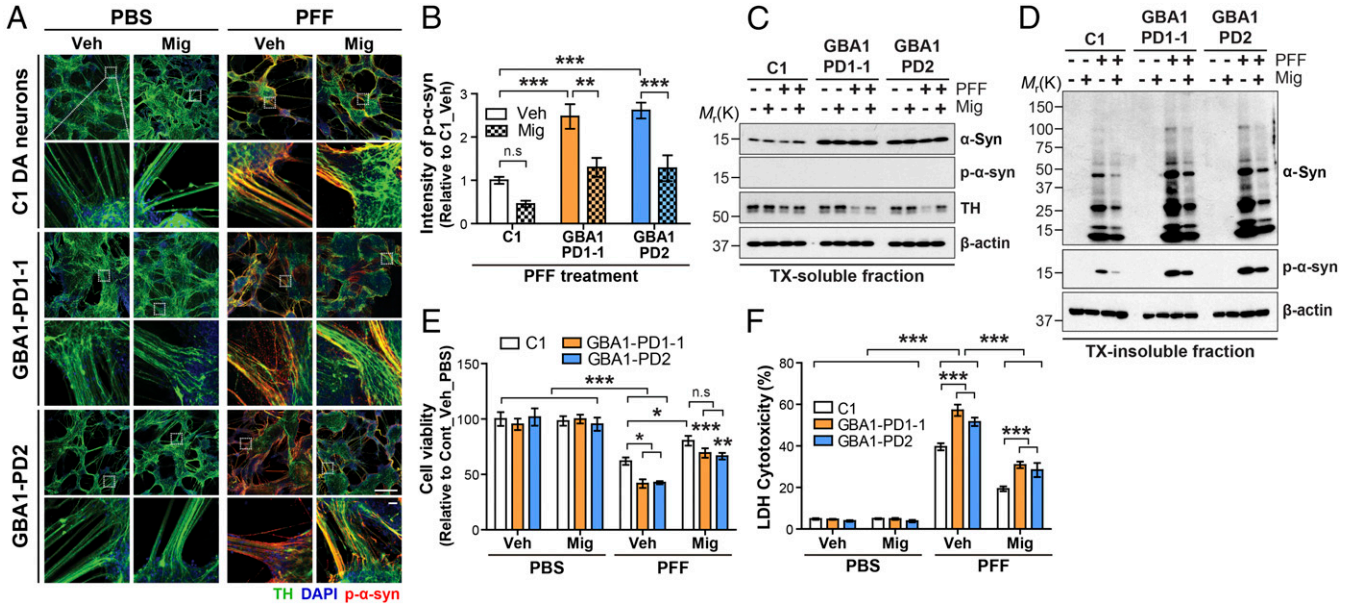

Fig. 5. PFF-induced pathology in GBA1-PD hDA neurons is reduced by miglustat treatment. (*A*) Fluorescent analysis of p-α-syn levels and TH staining in 5 μg/mL PFF-treated hDA neurons for 10 d without or with 100 μM miglustat treatment for 3 d before adding PFF. The images were generated by the tile scan algorithm in the Zen software (Carl Zeiss). [Scale bars, 100 μm for low magnification (*Upper*, 40×, 8 × 8 tile image) and 50 μm for high magnification (*Lower*, cropped image from low-magnification image.] (*B*) Quantification of p-α-syn levels for *A* ($n = 6$). (*C* and *D*) Control and GBA1-PD hDA neurons were sequentially fractionated in 1% Triton X-100 (TX-soluble) followed by 2% SDS (TX-insoluble) 14 d after 5 μg/mL PFF treatment. Western blots from (*C*) TX-soluble and (*D*) TX-insoluble fractions with or without 100 μM miglustat-treated hDA neurons using anti–α-Syn, anti-TH, anti–p-α-syn, and anti–β-actin antibodies. (*E* and *F*) Cell death in 5 μg/mL PFF-treated hDA neurons for 14 d without or with 100 μM miglustat treatment for 3 d before adding PFF was assessed using (*E*) AlamarBlue ($n = 6$) and (*F*) LDH cytotoxicity assay ($n = 5$). The error bars represent SEM. $^*P < 0.05$; $^{**}P < 0.01$; $^{***}P < 0.001$; n.s., not significant.

by PFF treatment in hDA neurons through AlamarBlue and lactate dehydrogenase (LDH) assays. PFF treatment for 2 wk induces neuronal toxicity in control and GBA1-PD hDA neurons. There is a greater neuronal toxicity in GBA1-PD hDA neurons treated with PFF compared with that in PFF-treated control hDA neurons (Fig. 5 *E* and *F*). Importantly, the enhanced PFF-induced neuronal toxicity in the GBA1-PD hDA neurons is significantly protected by treatment of miglustat (Fig. 5 *E* and *F*). Similar results are observed in hDA neurons augmenting GBA1 protein via lentiviral transduction (*SI Appendix*, Fig. S13). Taken together, these data indicate that lowering pathogenic GSL accumulation stabilizes α-syn tetramers and related multimers with a decrease in free monomers, which is protective.

Discussion

Pathogenic aggregation of α-syn is implicated in familial and sporadic PD and other synucleinopathies. It has long been believed that α-syn exists as a natively unfolded monomer of 14 kDa but can assemble into higher ordered multimers with α-helical structure upon binding to lipid vesicles in vitro (1, 2, 7, 31). Although still controversial (22, 32), recent studies revealed that endogenous α-syn occurs as a physiological helically folded tetramer of 60 kDa, which resists aggregation and toxicity in intact cells (9, 10). Our finding confirms and extends these results by showing that GBA1 deficiency and accumulation of GSLs due to GBA1 depletion and mutations lead to destabilization of the α-syn tetramers and related multimers and accumulation of monomers in SH-SY5Y cells, with GBA1 depletion and hDA neurons differentiated from human PD-iPSC with a heterozygous *GBA1* mutation (N370S/WT) (Figs. 1 and 3). Additionally, we find that treatment with miglustat to reduce the rate of GlcCer synthesis or augmentation of GBA1 protein to increase GBA1 enzymatic activity significantly reverses the GBA1 deficiency-induced destabilization of α-syn tetramers and related multimers and thereby protects against PFF-induced hDA neuronal toxicity.

Given that the lipid-binding motifs of α-syn are important for tetramer formation and disrupting these motifs decreases tetramers and causes PD-like neurotoxicity (11, 12), it can be speculated that lipid binding is essential for sustaining the α-syn tetramers in intact cells. Importantly, the α-syn tetramers have a high α-helix content and strongly bind to lipids (9). Our data suggest that accumulation of GlcCer due to GBA1 deficiency reduces the formation and/or stability of α-syn tetramers and related multimers (Figs. 1 and 3). Moreover, reduction of α-syn tetramers and related multimers due to GBA1 deficiency appeared to be dependent on intracellular GSL levels. Furthermore, VPS35 knockdown does not alter the ratio of α-syn tetramers and related multimers to monomers (*SI Appendix*, Fig. S14), even though α-syn protein levels were increased by affecting lysosomal degradation of α-syn (33). Thus, it is likely that lipid homeostasis is required for sustaining the α-syn tetramers and related multimers and lipid dyshomeostatsis in the disease may destabilize the α-syn tetramers, leading to accumulation of free monomers, which then misfold and contribute to pathological α-syn aggregation and neurotoxicity in PD.

The intact cell cross-linking method allowed us to detect α-syn tetramers and related multimers, while DJ-1 and TH, which are multimerized constitutively in cells, enabled us to confirm the general effectiveness of this method (24, 34). Although cross-linking of α-syn led to more high-molecular weight smears compared with DJ-1 and TH, it could be due to the 80 kDa species of α-syn, which is unstable to heat and/or sonication (23). Consistent with previous α-syn cross-linking patterns of tetramers and related multimers (9, 11, 12, 23), 60 kDa species of α-syn tetramers were trapped with more than 80 and 100 kDa species of α-syn multimers in primary murine cortical neurons and hDA neurons (Fig. 3*E* and *SI Appendix*, Fig. S3*A*). On the other hand, different patterns of α-syn tetramers and related multimers were observed in human neuroblastoma SH-SY5Y cells (Fig. 1*A*), which may be due to differences of proliferating property and/or insufficient differentiation to neurons (35). Interestingly, endogenous DJ-1 protein levels were unexpectedly increased in GBA1 KO cells, *GBA1* L444P het primary neurons, and GBA1-PD hDA neurons (Figs. 1 and 3 and *SI Appendix*, Fig. S3). Mitochondria in GBA1-deficient cells producing increased

reactive oxygen species, which leads to a functional defect of the respiratory chain (21), possibly up-regulates DJ-1 expression to attenuate oxidative stress (36). Moreover, chaperone-mediated autophagy plays a role in DJ-1 turnover through the lysosome (37). Thus, lysosomal dysfunction due to GBA1 deficiency may affect DJ-1 turnover and accumulation.

In summary, our results suggest that lipid dyshomeostasis by GBA1 deficiency leads to decreased α-syn tetramers and increased α-syn monomers, which may provide the building blocks for phospho-Ser129–positive aggregates in GBA1-PD iPSC-derived hDA neurons. Controlling the composition of the membrane lipid by the GSL reducing agent, miglustat reduced the destabilization of the α-syn tetramers and related multimers, PFF-induced aggregation, and toxicity (Figs. 2, 4, and 5). Maintaining the ratio of α-syn tetramers and related multimers to monomers by prevention of lipid dyshomeostasis could offer new neuroprotective therapeutic strategies to treat PD.

Materials and Methods

Intact Cell Cross-Linking. GBA1 KO cells, mouse primary cortical neurons, and hDA neurons were suspended in PBS (pH 8.0) followed by three washes with PBS (pH 8.0). Washed cells were incubated in 1 mM DSG for 30 min at 37 °C with 500 rpm shaking in Eppendorf ThermoMixer C. This reaction was quenched with 20 mM Tris (pH 7.4) for 15 min at room temperature. Complete protease inhibitor mixture (Roche) was added to DSG–cross-linked cells followed by sonication for 15 s (1 s pulse on/off) at 10% amplitude (Branson Digital sonifier). After sonication, the cell lysates were centrifuged at 100,000 × *g* at 4 °C for 1 h. The generation of GBA1 KO cells, primary cortical neuronal cultures, and detailed biochemical studies are described in *SI Appendix, SI Materials and Methods*.

Transgene-Free iPSC Generation. Six iPSC lines were generated from the skin fibroblast of control and heterozygous N370S GBA1-PD obtained from the Coriell Institute for Medical Research (*SI Appendix*, Table S1). All experiments using human stem cells were monitored by The Johns Hopkins University Institutional Stem Cell Research Oversight Committee. Further characterization and differentiation procedures are described in *SI Appendix, SI Materials and Methods*.

Statistical Analysis. Student's *t* test was used in GBA1 KO characterization. One-way ANOVA with Tukey's post hoc test was used for immunostaining quantification of GlcCer, the ratio of multimers to monomer in hDA neurons and miglustat-treated GBA1 KO cells, GBA1 enzymatic activity, dopamine release, and lipidomics. Two-tailed *t* test was used for the comparison of recording data of electrophysiology. Two-way ANOVA with Bonferroni post hoc test was used for immunoblotting quantification of hDA neuron differentiation, the ratio of multimers to monomer in miglustat-treated and LV-GBA1–transduced hDA neurons, p-α-syn staining quantification, and cell death assay. Assessments with $P < 0.05$ were considered significant. Statistical calculations were performed with GraphPad Prism software, Version 5.0 (www.graphpad.com).

ACKNOWLEDGMENTS. This work was supported by Maryland Stem Cell Research Foundation Grants 2012-MSCRFE-0059 and 2007-MSCRFI-0420-00; NIH/National Institute of Neurological Disorders and Stroke Grants 1RC2NS07027, 1U24NS078338, NS082205, NS098006, AR070751, NS093213, P50 AG005146, and P50 NS38377; the Morris K. Udall Parkinson's Disease Research Center; and the Jeffry M. and Barbara Picower (JPB) Foundation. The authors acknowledge the joint participation by the Adrienne Helis Malvin Medical Research Foundation and the Diana Helis Henry Medical Research Foundation through its direct engagement in the continuous active conduct of medical research in conjunction with The Johns Hopkins Hospital and the Johns Hopkins University School of Medicine and the Foundation's Parkinson's Disease Program H-1, H-2013. T.M.D. is the Leonard and Madlyn Abramson Professor in Neurodegenerative Diseases.

1. Dettmer U, Selkoe D, Bartels T (2016) New insights into cellular α-synuclein homeostasis in health and disease. *Curr Opin Neurobiol* 36:15–22.
2. Burré J (2015) The synaptic function of α-synuclein. *J Parkinsons Dis* 5:699–713.
3. Wright PE, Dyson HJ (2015) Intrinsically disordered proteins in cellular signalling and regulation. *Nat Rev Mol Cell Biol* 16:18–29.
4. Jensen PH, Nielsen MS, Jakes R, Dotti CG, Goedert M (1998) Binding of alpha-synuclein to brain vesicles is abolished by familial Parkinson's disease mutation. *J Biol Chem* 273: 26292–26294.
5. Outeiro TF, Lindquist S (2003) Yeast cells provide insight into alpha-synuclein biology and pathobiology. *Science* 302:1772–1775.
6. Logan T, Bendor J, Toupin C, Thorn K, Edwards RH (2017) α-Synuclein promotes dilation of the exocytotic fusion pore. *Nat Neurosci* 20:681–689.
7. Burré J, Sharma M, Südhof TC (2014) α-Synuclein assembles into higher-order multimers upon membrane binding to promote SNARE complex formation. *Proc Natl Acad Sci USA* 111:E4274–E4283.
8. Wang L, et al. (2014) α-Synuclein multimers cluster synaptic vesicles and attenuate recycling. *Curr Biol* 24:2319–2326.
9. Bartels T, Choi JG, Selkoe DJ (2011) α-Synuclein occurs physiologically as a helically folded tetramer that resists aggregation. *Nature* 477:107–110.
10. Wang W, et al. (2011) A soluble α-synuclein construct forms a dynamic tetramer. *Proc Natl Acad Sci USA* 108:17797–17802.
11. Dettmer U, et al. (2015) Parkinson-causing α-synuclein missense mutations shift native tetramers to monomers as a mechanism for disease initiation. *Nat Commun* 6:7314.
12. Dettmer U, Newman AJ, von Saucken VE, Bartels T, Selkoe D (2015) KTKEGV repeat motifs are key mediators of normal α-synuclein tetramerization: Their mutation causes excess monomers and neurotoxicity. *Proc Natl Acad Sci USA* 112:9596–9601.
13. Brady RO, Kanfer J, Shapiro D (1965) The metabolism of glucocerebrosides. I. Purification and properties of a glucocerebroside-cleaving enzyme from spleen tissue. *J Biol Chem* 240:39–43.
14. Sidransky E, et al. (2009) Multicenter analysis of glucocerebrosidase mutations in Parkinson's disease. *N Engl J Med* 361:1651–1661.
15. Nalls MA, et al. (2013) A multicenter study of glucocerebrosidase mutations in dementia with Lewy bodies. *JAMA Neurol* 70:727–735.
16. Gegg ME, et al. (2012) Glucocerebrosidase deficiency in substantia nigra of Parkinson disease brains. *Ann Neurol* 72:455–463.
17. Schöndorf DC, et al. (2014) iPSC-derived neurons from GBA1-associated Parkinson's disease patients show autophagic defects and impaired calcium homeostasis. *Nat Commun* 5:4028.
18. Farfel-Becker T, et al. (2014) Neuronal accumulation of glucosylceramide in a mouse model of neuronopathic Gaucher disease leads to neurodegeneration. *Hum Mol Genet* 23:843–854.
19. Sardi SP, et al. (2011) CNS expression of glucocerebrosidase corrects alpha-synuclein pathology and memory in a mouse model of Gaucher-related synucleinopathy. *Proc Natl Acad Sci USA* 108:12101–12106.
20. Mazzulli JR, et al. (2011) Gaucher disease glucocerebrosidase and α-synuclein form a bidirectional pathogenic loop in synucleinopathies. *Cell* 146:37–52.
21. Osellame LD, et al. (2013) Mitochondria and quality control defects in a mouse model of Gaucher disease–Links to Parkinson's disease. *Cell Metab* 17:941–953.
22. Fauvet B, et al. (2012) α-Synuclein in central nervous system and from erythrocytes, mammalian cells, and Escherichia coli exists predominantly as disordered monomer. *J Biol Chem* 287:15345–15364.
23. Dettmer U, Newman AJ, Luth ES, Bartels T, Selkoe D (2013) In vivo cross-linking reveals principally oligomeric forms of α-synuclein and β-synuclein in neurons and non-neural cells. *J Biol Chem* 288:6371–6385.
24. Wilson MA, Collins JL, Hod Y, Ringe D, Petsko GA (2003) The 1.1-A resolution crystal structure of DJ-1, the protein mutated in autosomal recessive early onset Parkinson's disease. *Proc Natl Acad Sci USA* 100:9256–9261.
25. Elstein D, et al. (2004) Sustained therapeutic effects of oral miglustat (Zavesca, N-butyldeoxynojirimycin, OGT 918) in type I Gaucher disease. *J Inherit Metab Dis* 27: 757–766.
26. Takahashi K, et al. (2007) Induction of pluripotent stem cells from adult human fibroblasts by defined factors. *Cell* 131:861–872.
27. Alcalay RN, et al. (2015) Glucocerebrosidase activity in Parkinson's disease with and without GBA mutations. *Brain* 138:2648–2658.
28. Woodard CM, et al. (2014) iPSC-derived dopamine neurons reveal differences between monozygotic twins discordant for Parkinson's disease. *Cell Rep* 9:1173–1182.
29. Bandaru VV, et al. (2013) A lipid storage-like disorder contributes to cognitive decline in HIV-infected subjects. *Neurology* 81:1492–1499.
30. Mao X, et al. (2016) Pathological α-synuclein transmission initiated by binding lymphocyte-activation gene 3. *Science* 353:aah3374.
31. Davidson WS, Jonas A, Clayton DF, George JM (1998) Stabilization of alpha-synuclein secondary structure upon binding to synthetic membranes. *J Biol Chem* 273: 9443–9449.
32. Burre J, et al. (2013) Properties of native brain alpha-synuclein. *Nature* 498:E4–E6; discussion E6–E7.
33. Tang FL, et al. (2015) VPS35 in dopamine neurons is required for endosome-to-golgi retrieval of Lamp2a, a receptor of chaperone-mediated autophagy that is critical for α-synuclein degradation and prevention of pathogenesis of Parkinson's disease. *J Neurosci* 35:10613–10628.
34. Goodwill KE, et al. (1997) Crystal structure of tyrosine hydroxylase at 2.3 A and its implications for inherited neurodegenerative diseases. *Nat Struct Biol* 4:578–585.
35. Encinas M, et al. (2000) Sequential treatment of SH-SY5Y cells with retinoic acid and brain-derived neurotrophic factor gives rise to fully differentiated, neurotrophic factor-dependent, human neuron-like cells. *J Neurochem* 75:991–1003.
36. Lu HS, et al. (2012) Hypoxic preconditioning up-regulates DJ-1 protein expression in rat heart-derived H9c2 cells through the activation of extracellular-regulated kinase 1/2 pathway. *Mol Cell Biochem* 370:231–240.
37. Wang B, et al. (2016) Essential control of mitochondrial morphology and function by chaperone-mediated autophagy through degradation of PARK7. *Autophagy* 12: 1215–1228.